Proceedings of the 2016 IEEE
International Conference on Robotics and Biomimetics
Qingdao, China, December 3-7, 2016

3D Printed Soft Gripper for Automatic Lunch Box Packing

Zhongkui Wang, Damith Suresh Chathuranga, and Shinichi Hirai

Abstract— **In this paper, we proposed a 3D printed soft robot gripper with modular design for lunch box packing. The gripper consists of a rigid base and three soft fingers. A snap-lock mechanism was designed for easy attach-detach assembly of the gripper without using screws. All components were 3D printed and the soft finger structure is based on the principle of fluidic elastomer actuator. Three finger designs, and soft gripper grasping and lifting deformable objects were investigated through finite element (FE) analysis and experiments. Results suggested that different finger designs yielded different curvature along the finger and generated different stress distribution once pressurized. The proposed gripper could grasp and lift objects with variable shapes and softnesses.**

(a) (b)

Fig. 1. A box lunch (a) and two cup containers (b) with different sizes.

I. INTRODUCTION

In Japan, eating box lunch (obento) is very popular due to its convenience and great variety. Every day, several million box lunches are produced and consumed in Japan. However, packing these lunch boxes is still performed by humans due to the fragility, variety, and high deformability of the food materials [1]. To reduce the labor costs, automation systems of lunch box packing are highly demanded by food industry.

A lunch box (Fig. 1a) normally consists of several small dishes distributed in waterproof cup containers. The cup container (Fig. 1b) is highly deformable and has a frustum shape with a smaller circular area on the bottom. Handling such a cup container filled with food materials is a challenging task because of the irregular shape and deformability of the food materials. The traditional rigid grippers and vacuum packing system, which have been widely used in food industry, have difficulties to fulfill this task because the rigid gripper may damage the food material and the vacuum system requires a flat surface to realize a suction. New grasping strategies are expected to well cope with this task. A robot gripper filled with magnetorheological (MR) fluid was proposed to grasp natural food products, such as apples, carrots, and broccolis [2]. The gripper did not perform well for grasping broccoli due to the spongy character. Another gripper proposed in [1] consists of four fingers and a tension-sensitive elastic thread to bind the container. This gripper can cope with the deformability and variable shapes of the containers by wrapping the elastic thread around the container. Meanwhile the conductive elastic thread works as a force sensor to measure the applied force during grasping. Unfortunately, the design and manufacture of the gripper is relatively complex.

In recent years, soft elastomer robot grippers have drawn great attention in many applications due to its characteristic of high compliance and resilience. Developments of soft gripper can date back to the 90s. Suzumori *et al.* first proposed a flexible microactuator driven by electro-pneumatic system and this small cylindrical actuator can realize pitch, yaw, and stretch motions [3]. A recent review in [4] summarized the design, fabrication, and control of soft robots. It states that soft robots provide an opportunity to bridge the gap between machines and people. More specifically for soft fluidic elastomer robots, Marchese *et al.* introduced the details of design and fabrication in [5]. According to [5], soft fluidic elastomer robots can be divided into three types: ribbed, cylindrical, and pleated, based on the actuator morphology. The grippers proposed in this paper is based on the pleated type morphology. The idea and design were previously introduced in [5], [6], [7] and was extended in [8] by adding a bend sensor to measure the curvature of the actuator. One downside of these grippers is the relatively complex fabrication process which includes several molding processes, assembling, and wax melting.

In this work, we present 3D printed soft grippers for grasping and lifting a cup container filled with food materials. Three finger designs were explained in Section II, followed by the FE analysis of single finger bending and three-finger grasping in Section III. The fabrication and assembly of the grippers were presented in Section IV, followed by the grasping experiments in Section V. The paper was concluded in Section VI with suggestions of future work.

II. DESIGN OF THE FINGER AND GRIPPER

When humans try to pick up a cup container filled with peanuts (Fig. 2), we tend to use all five fingers (Fig. 2a), which requires minimal effort to achieve a stable grasping. Using three fingers (Fig. 2b), we can also lift up the container with some effort and the container was deformed more significantly compared with five-finger grasping. Based on our experiences, it is not always possible to pick up the

The Authors are with Soft Robotics Laboratory, Department of Robotics, Ritsumeikan University, 525-8577 Kusatsu, Japan {wangzk at fc, hirai at se}.ritsumei.ac.jp

(a) (b) (c)

Fig. 2. Cup container filled with peanuts grasped by a human hand with (a) five fingers, (b) three fingers, and (c) two fingers.

container with only two fingers (Fig. 2c). Even in the case of successful lift, the large deformation generated on the container is not always acceptable. In this work, we proposed the grippers including three fingers with a modular design for easy assembly and replacement. If a three-finger gripper works well for the task, we believe that adding more fingers will increase the grasping stability.

The single finger was designed with a size of 82 mm (length) × 16 mm (width) × 15 mm (height). Three different finger designs (Fig. 3) were investigated. The design No. 1 (Fig. 3a) includes eleven smaller chambers and one bigger chamber at the end of the finger. The smaller chambers have a wall thickness of 1 mm and the larger chamber has a wall thickness of 3 mm. This makes the finger end stiffer than the rest part of the finger to mimic the function of the human nail. The design No. 1 is supposed to generate an uniform curvature along the finger length. To mimic human finger structure with distal joints, we proposed the design No. 2 (Fig. 3b) which includes two links and six small chambers mimicking two human distal joints. To investigate finger with varying curvature, we proposed the design No. 3 (Fig. 3c) in which the finger consists of three regions with different material properties. Among the three materials, the material 1 is the hardest and material 2 is the softest. To increase the grasping stability and mimic the human fingerprint, rippled structure was designed on the bottom surface.

For easy assembly, we designed a connector (Fig. 4a) and a base (4b). The connector is 3D printed simultaneously

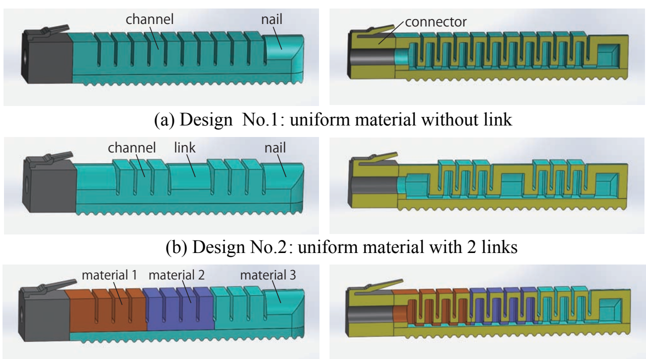

(a) Design No.1: uniform material without link

(b) Design No.2: uniform material with 2 links

(c) Design No.3: non-uniform material without link

Fig. 3. Three different designs of the soft finger. Different colors indicate materials with different elasticities.

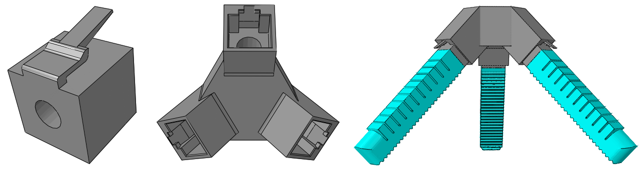

(a) (b) (c)

Fig. 4. The 3D designs of (a) the connector and (b) the base. Sub-figure (c) shows the assembled view of the gripper with three soft fingers.

with the soft finger. A hole with a diameter of 6 mm was designed on the connector to insert air hose. A snap-lock mechanism with male (on the connector) and female (on the base) interfaces was designed for connecting the connector to the base without using screws. Three female interfaces were distributed circularly in equal spacing on the base (Fig. 4b). Figure 4c shows the assembled gripper. The fingers were angled 45° vertically to form an initial gesture.

III. FE Analysis of the Finger and Gripper

FE analysis is a common computational tool for mechanical engineering and has been widely used in strength analysis of rigid mechanical parts. In recent years, FE analysis has also been used for design, analysis, and even control of soft robots [9], [10], [11]. Since the dynamics of soft robot system is difficult to be determined analytically, FE analysis becomes an important way to investigate the principles behind soft robot system. In this work, we performed FE analysis of the soft fingers and grippers using commercial FE package Abaqus®. The 3D models presented in the last Section were imported into Abaqus® and all parts were meshed with tetrahedron element. Interaction among the chamber surfaces were defined as tangential contact with a friction coefficient of 1.16, which is a typical value for rubber and rubber contact. Pressure loading was imposed on the chamber internal surfaces to actuate the bending.

The elasticities (indicated by Young's modulus) of the soft materials used in the FE simulation were listed in Table I. The material names and the Shore hardness values are referred to the multi-material datasheet of the Objet Connex 3D printer. The values of Young's modulus, which is usually required for FE simulation, were calculated using the following equation [12]

$$E = \frac{0.0981(56+7.66s)}{0.137505(254-2.54s)},$$

TABLE I

Material properties used in the soft fingers

Material No.	Material name	Shore hardness A	Young's Modulus (MPa)	Average (MPa)
Material 1	DM_9860	57-63	3.22-4.09	3.65
Material 2	DM_9840	35-40	1.40-1.70	1.55
Material 3	DM_9850	45-50	2.05-2.46	2.25

where E denotes the Young's modulus and s denotes the Shore hardness. The average values listed in Table I were used in the FE simulations. In addition, we set the Poisson's ratio to 0.49 since rubber material is usually incompressible.

A. *Simulation Results of Single Finger*

Figure 5 shows the simulation results of single finger under gravity and different air pressure loadings. The unloaded finger is configured in a horizontal position and the loadings were impose in two steps. In the first step, only gravity was imposed on the FE model and the deformation under gravity was simulated as shown at the top of Figs. 5a, 5c, and 5e. Air pressure loading was imposed during the second step and simulation results were given in Figs. 5b, 5d, and 5f. Stress distributions inside the chambers were given at the bottom of Figs. 5a, 5c, and 5e. To quantitatively compare the results, we obtained three quantities from the simulation results: (1) the gravity bend defined as the vertical displacement of the finger tip under gravity, (2) the bending angle defined as the angle α in Fig. 5f during pressure loading, and (3) the maximum stress during pressure loading. The three values

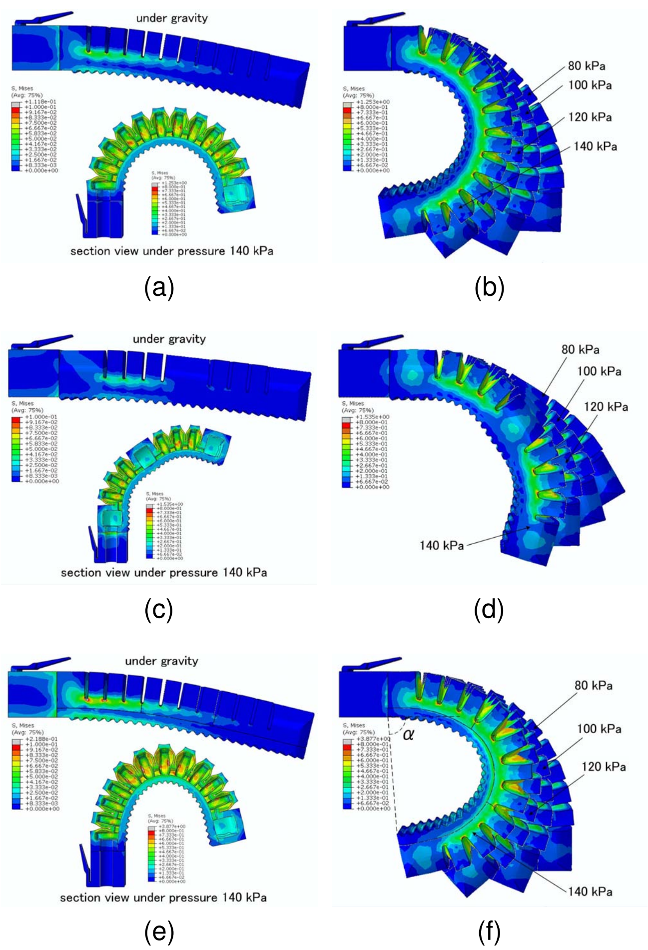

Fig. 5. Simulation results of different finger designs. Sub-figures (a), (c), and (e) show the designs No.1, No.2, and No.3 under gravity, and the section view under pressure of 140 kPa. Sub-figures (b), (d), and (f) show the comparisons of the designs No.1, No.2, and No.3 under different pressures of 80 kPa, 100 kPa, 120 kPa, and 140 kPa.

TABLE II
COMPARISONS OF THREE MEASUREMENTS FROM SIMULATION RESULTS

Design No.	Gravity bend (mm)	Air pressure loading (kPa)	Bending angle (°)	Max stress (MPa)
No. 1	13.13	80	52.37	0.69
		100	65.81	0.87
		120	80.26	1.06
		140	96.89	1.25
No. 2	8.31	80	31.46	0.81
		100	38.67	1.03
		120	46.32	1.28
		140	57.26	1.53
No. 3	14.06	80	48.38	1.62
		100	59.58	2.13
		120	71.80	2.80
		140	86.63	3.88

were listed in Table II for comparisons. We found that the design No. 2 behaves stiffer with less bending under gravity and pressure loadings compared with the other two designs. This is because the design No. 2 has less chambers compared with the other two designs. The design No. 3 generates larger gravity bend because it has a softer region (material 2) in the middle. Under pressure loadings, design No. 1 generates the largest bending angle comparing with the rest two designs. Compared with design No. 1, design No. 3 generates less bending angle because the stiff region (material 3) near the base. From Fig. 5, we also found that the design No. 1 generates uniform curvature, design No. 2 generates bending at the joint regions, and design No. 3 is able to generate non-uniform curvature along the finger length. Meanwhile, we found that the maximum stress did not differ much between designs No. 1 and No. 2, but much larger stress was found in design No. 3. Large stress was found at the middle region where the softer material was distributed (Fig. 5e). The stress distribution inside chambers (bottom of Figs. 5a, 5c, and 5e) is more uniform with design No. 1 compared to the other two designs.

B. *Simulations of Grasping and Lifting a Container*

Simulations of different grippers grasping and lifting a soft container were performed using the FE models and the simulation results were shown in Fig. 6. The soft container has similar shape and size as the paper container shown in Fig. 1b. The wall thickness of the container was modeled as 1 mm and the material property was set as the same as material 3. The container weights approximately 50 g just like the paper container filled with peanuts (Fig. 2). The friction coefficient between the fingers and the container surface is set to 0.65. A rigid plate was placed under the container. The simulation was divided into three steps: (1) gravity loading, (2) pressure loading, and (3) lifting motion. Figures 6b, 6c, and 6d showed the successful trials using different grippers with pressure loadings of 140 kPa, 180 kPa, and 140 kPa respectively. Grippers with design No. 1 and No. 3 could lift the container with a pressure of 140 kPa, but design No. 2 requires higher pressure of 180 kPa to successfully lift the container. This is because the finger

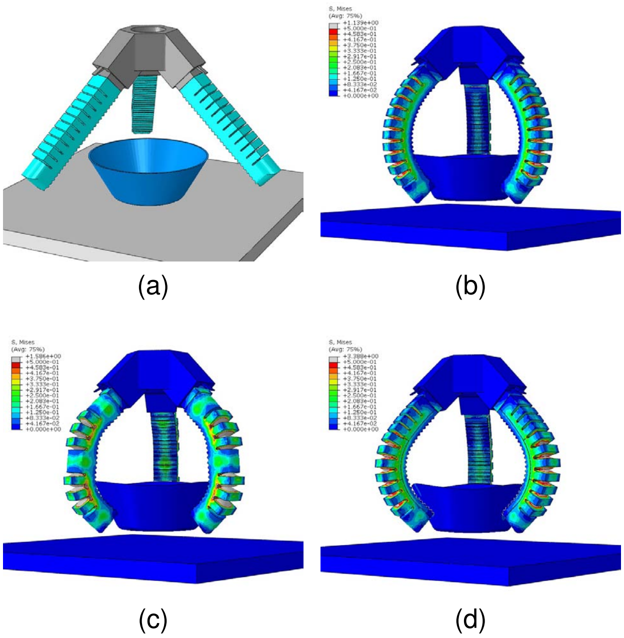

Fig. 6. Simulation results of different grippers grasping and lifting a soft container. Sub-figure (a) shows the initial configuration, and sub-figures (b), (c), and (d) show the final configurations after grasping and lifting the container with the finger designs No. 1, No. 2, and No. 3, respectively.

with design No. 2 requires a larger pressure to generate a similar bending angle compared with the other two designs. Different grippers formed different caging cavities depending on the bending behaviors of the finger. From simulation results, we found that gripper with design No. 1 fits the container shape better and generates less deformation on the container compared with the other two designs.

IV. Fabrication and Assembly Process

The grippers were printed using a state-of-the-art 3D printer (Objet260Connex$^{\text{TM}}$ system). This printer can print 14 digital materials simultaneously with different mechanical properties by mixing a soft rubber-like (TangoBlack+) and a hard polypropylene-like (VeroWhite) material.

A single finger was printed as two separate parts (Fig. 7a): (1) the chambers together with the connector, and (2) the bottom cover to seal the chambers from leaking. After removing the support materials, the cover was glued onto the chambers to complete the finger construction (Fig. 7c). The materials used to print the soft regions of the fingers were listed in Table I. The material used to print the connector is DM_8525, which provides balanced elastic property for the snap-lock mechanism. The base (Fig. 7b) was printed with the hard material (VeroWhite). After plugging in the air hoses and inserting three fingers into the base, we have the assembled gripper (Fig. 7d) without using screws. It takes approximately 2 hours to print the two separate parts of the finger. Multiple fingers can be printed simultaneously as long as the parts can fit in the printer workspace (255 mm×252 mm×200 mm). It takes approximately 10 minutes to remove the support material, and 10 minutes to glue the two parts together.

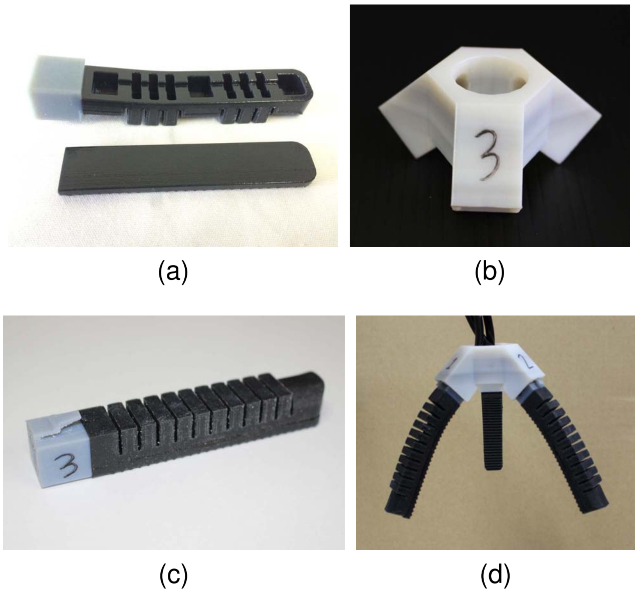

Fig. 7. Fabrication and assembly of the gripper. Sub-figure (a) shows the two printed parts of the finger, (b) the printed base, (c) the complete finger by gluing the two parts together, and (d) the assembled gripper.

V. Experiments

For preliminary experimental validations, we employed an air compressor (JUN-AIR 3-4) and an electro-pneumatic regulator (SMC® ITV2030) to generate constant air pressures. Experiments of single finger under different pressure loadings and gripper grasping the paper container filled with 50 grams peanuts were performed.

A. Single Finger Experiments

Figure 8 shows the experimental results of different finger designs under different loading conditions. The quantitative bending measurements were calculated and listed in Table III for comparisons. Under gravity, finger design No. 3 generates the largest bending and design No. 2 generates the smallest bending. This agrees with the FE simulation results. On the other hand, the bending amplitudes in experiments are much larger than the ones in simulation. Under pressure loadings, we found that the design No. 2 generates the

TABLE III
Bending measurements from experimental data

Design No.	Gravity bend (mm)	Air pressure loading (kPa)	Bending angle (°)
No. 1	28.98	20	61.39
		30	75.75
		40	89.35
		50	102.45
No. 2	23.81	20	38.15
		30	47.10
		40	58.64
		50	67.55
No. 3	32.54	20	56.69
		30	71.62
		40	89.94
		50	104.07

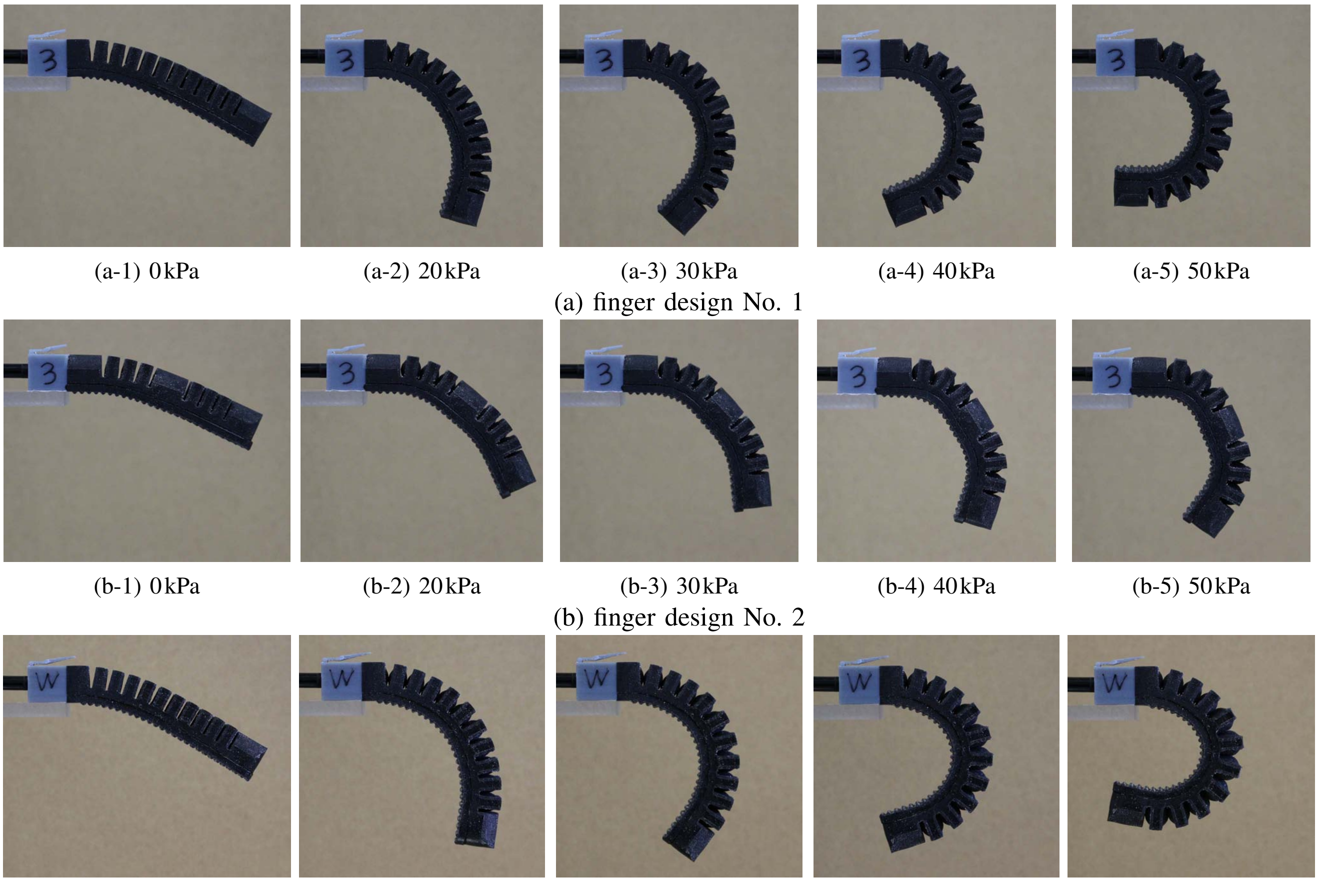

(a-1) 0 kPa (a-2) 20 kPa (a-3) 30 kPa (a-4) 40 kPa (a-5) 50 kPa

(a) finger design No. 1

(b-1) 0 kPa (b-2) 20 kPa (b-3) 30 kPa (b-4) 40 kPa (b-5) 50 kPa

(b) finger design No. 2

(c-1) 0 kPa (c-2) 20 kPa (c-3) 30 kPa (c-4) 40 kPa (c-5) 50 kPa

(c) finger design No. 3

Fig. 8. Experimental results of different finger designs under different loading conditions.

smallest bending angles among three designs. Design No. 1 generates larger angles when loading pressures are relatively low (20 kPa and 30 kPa), which agrees with the simulation results. With relatively high loading pressures (40 kPa and 50 kPa), design No. 3 generates slightly larger bending angles, which does not agree with the simulation results. We can also see that the design No. 3 forms the largest curvature among three designs. Regarding the loading pressures, we found that much less pressures were required in experiments to generate similar bending angles. We believe that these disagreements were caused by the material properties (Table I) used in simulations. Because the chamber walls are quite thin and the finger was highly deformed during bending, the traditional linear material property (Young's modulus) is no longer sufficient and material nonlinearity needs to be taken into account. This will be investigated in our future work. Nevertheless, the bending tendency from both simulation and experiment is consistent and this allows us to use simulation to instruct the design of the soft gripper.

B. Grasping and Lifting Experiments

Experiments of grasping and lifting a paper container filled with 50 g peanuts were conducted with the grippers. Pressure loadings ranging from 20 kPa to 60 kPa were imposed and successful lift is defined as 10 s hanging without dropping. Figure 9 shows the experimental snapshots of the initial state before loading and successful lifts for different finger designs. Using design No. 1 and No. 3, pressure of 40 kPa is enough to achieve a successful lift, but design No. 2 requires a pressure of 60 kPa to successfully lift the container. Large curvature was found in the gripper design No. 3. These also agreed with simulation results.

To test the grasping ability of the gripper, we conducted experiments using different objects, such as a smaller container filled with 50 g red beans and with a 36 g fried chicken, a 64 g wooden ball, and a 48 g raw egg. Successful lifts using the design No. 3 were shown in Fig. 10. We found that it is more difficult to lift the container filled with beans and it requires a higher pressure (50 kPa) compared with lifting the container with peanuts (Fig. 9). This is because the size of the bean container is smaller. Therefore, it requires larger bending to generate same grasping and lifting force. Same situation happens when we grasp and lift the wooden ball compared with the raw egg. It is more difficult to lift the smaller egg than the wooden ball. We also found that it is relatively easier to grasp and lift a rigid object, such as the wooden ball and the egg, compared with soft ones due to the deformation during lifting.

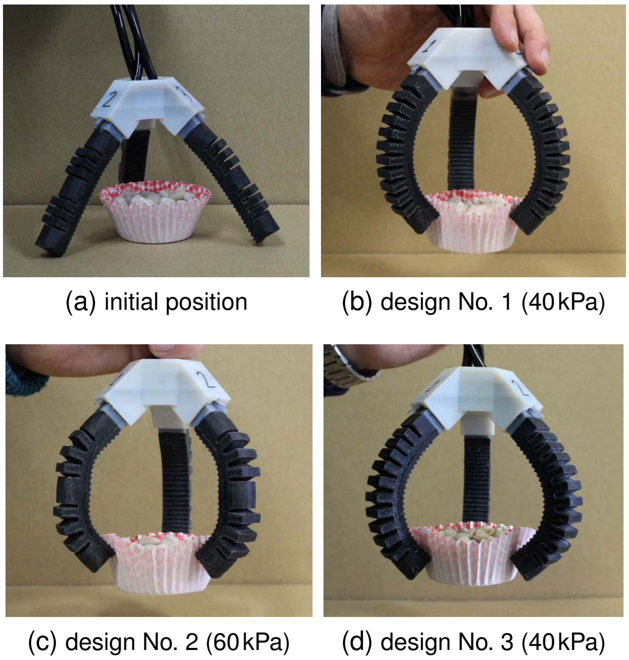

(a) initial position (b) design No. 1 (40 kPa)

(c) design No. 2 (60 kPa) (d) design No. 3 (40 kPa)

Fig. 9. Snapshots of the grasping and lifting experiments. Sub-figure (a) shows the initial state, and (b), (c), and (d) show the successful lifts for different finger designs.

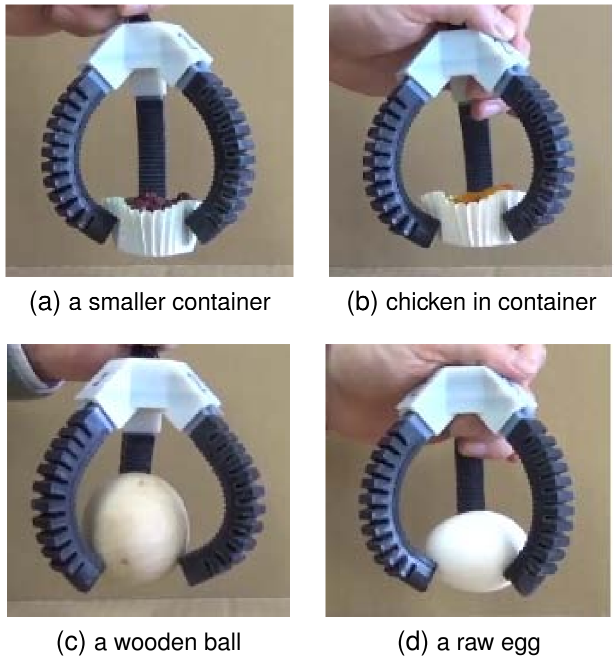

(a) a smaller container (b) chicken in container

(c) a wooden ball (d) a raw egg

Fig. 10. Experimental snapshots of grasping and lifting (a) a smaller paper container filled with red beans, (b) a fried chicken in a paper container, (c) a wooden ball, and (d) a raw egg.

VI. CONCLUSIONS

In this paper, we proposed a 3D printed soft gripper for the purpose of automating lunch box packing in Japan. The finger design is based on the principle of fluidic elastomer actuator. The gripper has a modular design and a snap-lock mechanism was designed for easy assembly without using screws. All parts were 3D printed and the fabrication process is relatively simple and efficient. Three finger designs were proposed and investigated through FE analysis and experimental validations. We found that the finger with links (No. 2) required larger pressure to generate a similar curvature. The finger constructed by 3 materials (No. 3) could create varying curvature along the finger, but it resulted in larger stress inside the chamber. The gripper with three fingers could successfully grasp and lift variable kinds of objects, including deformable container filled with peanuts and beans, a wooden ball, and a raw egg. We found that it is relatively easier to grasp and lift a rigid and larger objects compared with soft and smaller ones. The main contributions are threefold: (1) development of the easy fabricated and assembled soft gripper, (2) FE analysis of soft finger and gripper grasping soft target, which provides a way to study soft robot dynamics, and (3) different finger designs, particularly the design No. 3, which suggested a possibility to make non-uniform soft robots.

Only preliminary results were presented in this paper. More quantitative analysis will be investigated in future work. Such analysis includes the relationship between the input pressure and the generated grasping force, the grasping force required to lift the container with food materials, the curvature changes during grasping, and so on. Future work also includes mounting the gripper on a robot arm to perform automatic grasping and lifting, and integrating sensors in the finger to achieve proprioceptive sensing.

REFERENCES

[1] H. Iwamasa, S. Hirai, “Bindling of food materials with a tension-sensitive elastic thread,” in Proc. IEEE International Conference on Robotics and Automation, Seattle, 2015, pp. 4298-303.

[2] A. Pettersson, S. Davis, J.O. Gray, *et. al.*, “Design of a magnetorheological robot gripper for handling of delicate food products with varying shapes,” Journal of Food Engineering, 98, 2010, pp. 332-8.

[3] K. Suzumori, S. Iikura, H. Tanaka, “Development of flexible microactuator and its applications to robotic mechanisms,” in Proc. IEEE International Conference on Robotics and Automation, Sacramento, 1991, pp. 1622-7.

[4] D. Rus, M. T. Tolley, “Design, fabrication and control of soft robots,” Nature 521, 2015, pp. 467-75.

[5] A. D. Marchese, R. K. Katzschmann, D. Rus, “A recipe for soft fluidic elastomer robots,” Soft Robotics, 2(1), 2015, pp. 7-25.

[6] C. D. Onal, D. Rus, “A modular approach to soft robots,” in Proc. the Fourth IEEE RAS/EMBS International Conference on Biomedical Robotics and Biomechatronics, Roma, 2012, pp. 1038-45.

[7] R. K. Katzschmann, A. D. Marchese, D. Rus, “Autonomous object manipulation using a soft planar grasping manipulator,” Soft Robotics, 2(4), 2015, pp. 155-64.

[8] B. S. Homberg, R. K. Katzschmann, M. R. Dogar, D. Rus, “Haptic identification of objects using a modular soft robotic gripper,” in Proc. IEEE/RSJ International Conference on Intelligent Robots and Systems, Hamburg, 2015, pp. 1698-705.

[9] C. Duriez, “Control of elastic soft robots based on real-time finite element method,” in Proc. IEEE International Conference on Robotics and Automation, Karlsruhe, 2013, pp. 3983-7.

[10] F. Largilliere, V. Verona, E. Coevoet, *et. al.*, “Real-time control of soft-robots using asynchronous finite element modeling,” in Proc. IEEE International Conference on Robotics and Automation, Seattle, 2015, pp. 2550-5.

[11] P. Polygerinos, Z. Wang, J. T. B. Overvelde, *et. al.*, “Modeling of soft fiber-reinforced bending actuators,” IEEE Transactions on Robotics, 31(3), 2015, pp. 778-89.

[12] I. M. Meththananda, S. Parker, M. P. Patel, M. Braden, “The relationship between Shore hardness of elastomeric dental materials and Young’s modulus,” Dental Materials, 25, 2009, pp. 956-9.